DESIGN OF AN ANALOG-DIGITAL PI CONTROLLER WITH GAIN SCHEDULING FOR LASER TRACKER SYSTEMS

Christian Wachten, Lars Friedrich, Claas Müller, Holger Reinecke
Department of Microsystems Technology, University of Freiburg, Georges-Koehler-Allee 103, 79110 Freiburg, Germany

Christoph Ament
Institue for Automation and Systems Engineering, TU Ilmenau, 98693 Ilmenau, Germany

Keywords: Laser tracker system, *PI* controller with µC, Analog-digital design, Absolute distance measurement.

Abstract: Laser trackers are important devices in position metrology. A moving reflector is tracked by a laser beam to determine its position in space. To ensure a proper function of the device the feedback control loop is an essential part. An analog *PI* controller with online parameter adaptation and absolute distance measurement ability is used to guarantee an optimal dynamic system. The feedback controller is connected to a quadrant detector which serves as the sensor element in the control loop. The position of an incoming laser beam is measured by the quadrant detector and the controller provides the input signals for a subsequent actuator. The control variable is the deviation of the laser beam from the centre of the diode which should ideally be zero. The actuator consists of two axes and each one is equipped with a rotatable mirror. The task of the controller is to rotate the mirrors in such a way so that the laser beam follows the movements of the reflector. To design an optimal controller linear, time-invariant models of the actuator and the position sensor are developed to optimize its parameters. The gain of the plant correlates with the distance between the reflector and the laser tracker. To achieve the optimal dynamic performance the controller is automatically adapted to the distance during operation. A method based on oscillation injection to measure the absolute distance is developed. Due to higher dynamic demands a standard analog *PI* controller is implemented with the controller gain tuned by digital potentiometers. A microcontroller is used to adjust the parameters and to estimate the distance. During the power up sequence and in case of a beam loss the system is completely controlled by the digital part.

1 INTRODUCTION

Laser trackers are devices which are used in position metrology and in calibration tasks due to their capability of doing static as well as dynamic high accuracy measurements (Riemensperger & Gottwald 1990). A HeNe laser with a Gaussian beam profile emits two light beams with different frequencies f_1 and f_2. These beams are divided by an interferometer into a reference beam and a measurement beam. The measurement beam leaves the interferometer and is deflected by the mirrors of an actuator in such a manner that it follows the movement of a retroreflector. The reflected light is analyzed by a position sensitive detector, the analog output signals of which are used to determine the position of the incoming beam. The reflected light beam also interferes with the reference beam in the interferometer. So, by measuring the two mirror angles of the actuator and the relative distance given by the interferometer the position of the reflector is calculated by using an analytical model. Figure 1 shows the operation principle.

An important part of the tracker is the feedback controller in the tracking unit. It provides the input signals for the actuator, so that the laser beam follows the movement of the retroreflector. The basic task of the controller is to guarantee the proper interferometer function. Dynamic aspects like a high velocity or high acceleration of the retroreflector with a low contouring error are also important.

We present the development of a fast and cost effective analog feedback controller for a tracking unit that can be used with laser tracker systems. The

Wachten C., Friedrich L., Müller C., Reinecke H. and Ament C. (2008).
DESIGN OF AN ANALOG-DIGITAL PI CONTROLLER WITH GAIN SCHEDULING FOR LASER TRACKER SYSTEMS.
In *Proceedings of the Fifth International Conference on Informatics in Control, Automation and Robotics - SPSMC*, pages 5-12
DOI: 10.5220/0001478600050012

tracking unit is designed for working with an interferometer but can also act as an autonomous system because of the integrated absolute distance measurement technique. A distance of about eight meters between the tracker unit and the reflector is easily achieved in experiment without static tracking errors. Furthermore, the lateral offset of the laser beam does not exceed a quarter of the beam diameter and thus guarantees stable interferometer functionality.

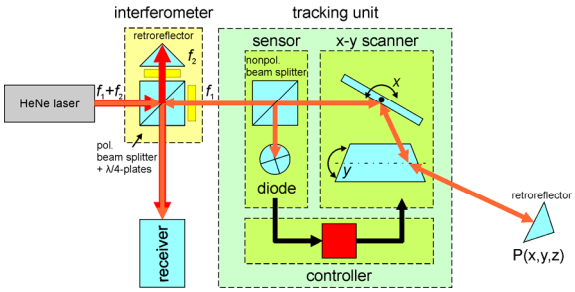

Figure 1: Operation principle of a laser tracker system. The frequency f_1 represents the measurement beam and f_2 the reference beam.

2 SYSTEM COMPONENTS

The tracking unit consists of three components (see figure 1). The first component is the sensor element which is a combination of a nonpolarizing beam splitter and a quadrant diode. The second component is a x-y scanner with two magnetically driven mirrors that deflect the laser beam (galvanometer scanner). The third component is the controller that connects the sensor element with the actuator.

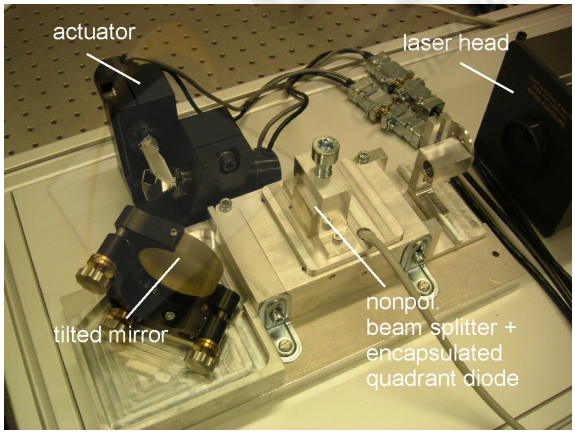

Figure 2: Photograph of the tracking unit. The two mirrors of the actuator deflect the incoming laser beam. A tilted mirror is used to adjust the light path.

The laser beam hits a nonpolarizing beam splitter. It has a division ratio of 50:50. Afterwards, it is deflected by the scanner and is then reflected by the retroreflector. The retroreflector has the unique property that the incoming laser beam is reflected into the same direction where it came from. On its returning path the reflected beam hits the nonpolarizing beam splitter again and a part of the beam is deflected on a quadrant diode. This diode provides the analog input voltages for the feedback controller since it has an integrated transimpedance amplifier. The feedback controller generates the input signals for the scanner. Ideally, the laser beam is centered on the diode and the position signals equal zero volts. By moving the reflector the laser beam leaves the center on the diode and the position signals change. The controller compensates the position change and modifies the input signals of the actuator. The two mirrors rotate and deflect the laser beam in such a way that the offset becomes zero. Figure 2 shows a photograph of the complete tracking unit.

2.1 Laser Head

The laser is a class II HeNe laser with a Gaussian beam profile. It emits two linear, orthogonal polarized beams with a split frequency of about 1.8 MHz. The beam diameter is about 6 mm. The power P of the laser is about 120 µW.

2.2 Magnetic Actuator

The magnetic actuator is a galvanometer scanner produced by Cambridge Technology. It has silver coated mirrors which allow a maximal beam aperture of 10 mm. Each mirror is magnetically driven and has its own analog *PID* controller to hold the desired position. The transfer factor is 0.83 V/° (mechanical) at the input side of the controller and 0.5 V/° (mechanical) at the output side of the position detector. Integrated sensors allow the measurement of the rotation angle of the mirrors. The short term stability is about 8 µrad. The maximal mechanical rotation angle is ± 12.5° limited by the used assembly.

2.3 Quadrant Photodetector

The sensor element of the tracking unit is a quadrant photodiode. Figure 3 shows a photograph of the photodiode and a sketch of its quadrants. Each quadrant is sensitive to light with a sensitivity that is specified to 0.54 A/W at a wavelength of 900 nm. The spacing

between the quadrants is 0.2 mm, the quadrant radius is 3.99 mm.

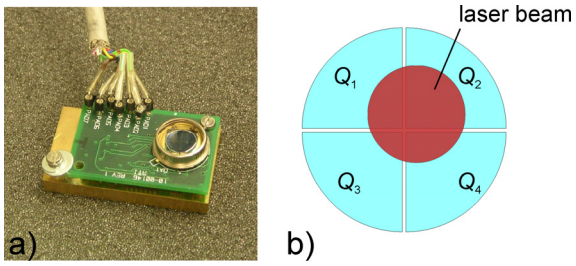

Figure 3: Photograph of the quadrant detector a) and sketch b) of its quadrants. The voltage level of the position signals depends on the area that is covered by the laser beam, its shape, its power and the wavelength.

The diode current depends on the power of the laser beam, its shape, its wavelength and the area that is covered. To perform a current to voltage transformation a transimpedance amplifier is put on the same circuit. The output of the amplifier consists of three voltages that completely define the position and the power of the laser beam. The signals can be calculated with the following formulas:

$$V_{Sum} = (I_1 + I_2 + I_3 + I_4) \cdot 10^4 \text{ V/A} \quad (1)$$

$$V_{TB} = ((I_1 + I_2) - (I_3 + I_4)) \cdot 10^4 \text{ V/A} \quad (2)$$

$$V_{LR} = ((I_1 + I_3) - (I_2 + I_4)) \cdot 10^4 \text{ V/A} \quad (3)$$

The symbol I_i represents the current of a quadrant Q_i. The signal V_{Sum} is the summation of the voltages that are generated by each quadrant and thus is an indicator for the total power of the incoming light beam at a known wavelength. The signal V_{TB}, the so called top-bottom voltage, represents the position of the laser beam in vertical direction. The signal V_{LR}, the so called left-right voltage, represents the position of the laser beam in horizontal direction. If for example the laser power is the same on each quadrant, V_{TB} and V_{LR} become zero volts.

3 MODELING OF THE PLANT

A block diagram of the system is shown in fig-ure 4. The output signal y of the system is the deviation of the light beam from the center of the quadrant diode. This deviation should become zero for each component. The output signal y is a superposition of the movement of the reflector and the compensation part of the actuator. The gain between the mirror angle and the movement of the light beam on the diode depends on the distance between the reflector and the tracking unit. This is modeled in the block "light path". The symbol z represents the position of the reflector in space and thus is a three-dimensional vector. The signal y represents the beam position on the diode area and thus is a two-dimensional vector.

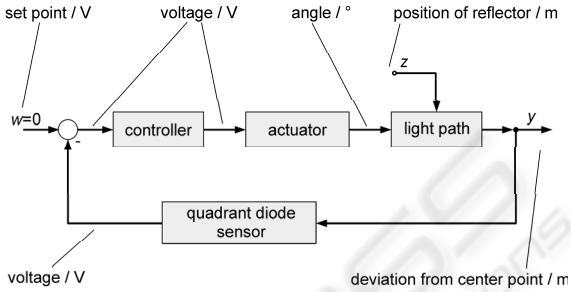

Figure 4: Block diagram of the plant. The different inputs and outputs with their units are shown.

To design an optimal feedback controller, models are developed and the model parameters are identified for the blocks "actuator", "quadrant diode" and "light path".

3.1 Modeling of the Block "actuator"

To obtain a transfer function for the magnetic actuator the step response is recorded for each axis monitoring the position output of the integrated angle encoders. A square wave with a peak-peak voltage of 100 mV (corresponding to an angle of about 0.06°) and a frequency of 30 Hz is applied to the inputs of the scanner.

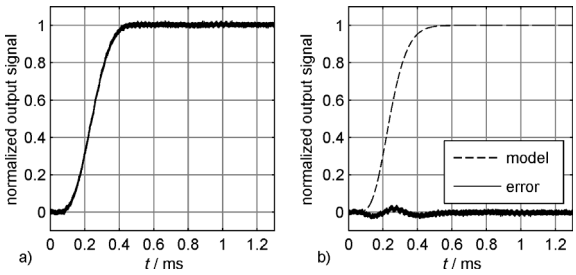

Figure 5: Normalized and averaged measurement a) of the step response of the y mirror and the model b) of the step response with its error. The step rises at t = 0 s.

Figure 5 shows the measured step response and the step response of the model for the y mirror. It is assumed that the scanner has PT_n behavior and thus can be modeled with a PT_n element in (4).

$$H_i(s) = \frac{K_i}{(1 + T_i \cdot s)^{n_i}}, \; i = x,y \quad (4)$$

The parameter K_i describes the gain and the parameter T_i represents the time constant for axis i. The parameter n_i stands for the order of the element. To obtain the parameters the method of the time percentage values is applied. Since the measurement is not supposed to have ideal PT_n behavior a least-squares fit is done to optimize the parameters so that the error between the model and the measurement becomes minimal. The start parameters for the optimization are the results given by the method of the time percentage values (Schwarze 1962). The final optimization yields in $n_y = 9$ and $T_y = 27.51$ µs for the y mirror. The parameters for the x mirror result in $n_x = 10$ and $T_x = 23.42$ µs. Taking into account that the gain between the output signal and the mechanical deflection is 0.5 V/° the gains are calculated to $K_x = 1.210$ °/V and $K_y = 1.207$ °/V, respectively. The -3 dB frequency is about 1.8 kHz (model).

3.2 Modeling of the Block "diode"

The time response of the diode can be modeled in the same way as the time response for the actuator. A red LED is used to generate the step response because it is fast enough and its time response can be neglected. The output signal V_{Sum} is measured. The LED has a power of about 7 µW. Figure 6 shows the measurement and the model of the step response.

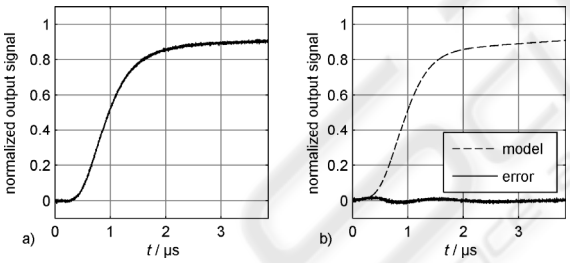

Figure 6: Normalized and averaged measurement a) of the step response of the diode and the model b) with its error. A red, pulsed LED is used to illuminate the active area. The step rises at t = 0 s.

The modeling with only a single PT_n element is not applicable because there is a steep increase of the signal until 1.6 µs. Afterwards, the signal increases very slowly and does not reach 100% even after 4 µs. Therefore, it can be shown that a good approximation is a combination of a PT_n element and a PT_1 element. This is done in (5).

$$H_D(s) = \frac{g}{(1+T_1 \cdot s)^{n_D}} + \frac{1-g}{1+T_2 \cdot s} \qquad (5)$$

The parameters T_1 and T_2 represent time constants of the two elements, the parameter g normalizes the output and the parameter n_D represents the order of the PT_n element. All parameters are obtained using a least squares fit so that the deviation of the model and the measurement becomes minimal. The optimal parameters are $n_D = 7$, $T_1 = 136$ ns, $T_2 = 4.75$ µs, $g = 0.793$. The model predicts a -3 dB frequency of 250 kHz.

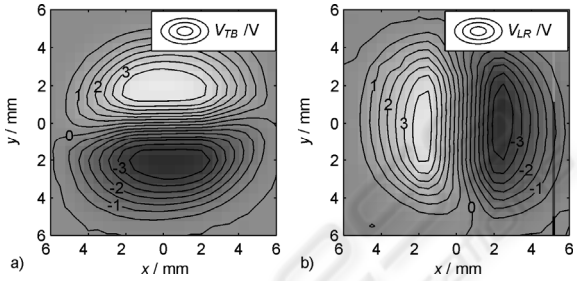

Figure 7: Local behavior of the diode. There is a nonlinear relation between the output voltage and the position of the beam.

Because the diode generates position signals not only the time response is important but also its local behavior. Figure 7 shows the local behavior of diode. The quadrant diode was put onto an x-y station and a laser diode with a power of 771 µW was installed in front of it. The station moves to 900 defined positions that are placed in an equally spaced square.

In figure 7 it can be seen that there is a nonlinear relation between the position and the output voltages. In the center of the diode the contour lines are nearly parallel to the corresponding axis and so a linearization is possible. It is obvious that the signal V_{TB} only depends on a movement in y direction and V_{LR} only depends on a movement in x direction. As a result, each axis of the scanner can be regarded as independent.

3.3 Modeling of the Block "light path"

The block "light path" depends on the position of the reflector. If the angular errors are neglected the reflector can be approximated as its center point in a plane (see figure 8a). The hitting point of the incoming laser beam is point reflected with the center. An offset between the incoming and the reflected laser beam can have different reasons, for example a rotation or a lateral displacement of the reflector.

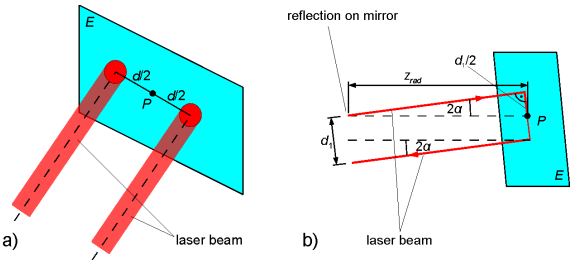

Figure 8: Modeling of the reflector. An incoming beam is reflected at the center of the reflector.

The first effect is shown in figure 8b. The mirror rotation angle is α. It is assumed that the reflector is z_{rad} away from the tracking unit. So the offset d_1 can be written as

$$d_1 = 2 \cdot z_{rad} \cdot \sin(2\alpha) \approx 4 \cdot z_{rad} \cdot \alpha \qquad (6)$$

The second effect resulting in a beam offset is the lateral displacement z_{lat} of the reflector. The indices represent the coordinate frame of the diode. So it can be written as

$$d_{2,i} = 2 \cdot z_{lat,i}\,,\ i = x,y \qquad (7)$$

The total deflection on the quadrant diode is a combination of these two effects as shown in (8)

$$y_i = d_1 + d_{2,i}\,,\ i = x,y. \qquad (8)$$

4 CONTROLLER DESIGN

The controller has to be designed separately for the x and the y-axis. Because of the decoupling of the axes shown in figure 7 the problem is reduced to the controller design for one axis. Exemplarily, the x-axis is used to demonstrate the design process. It can be derived from the block "light path" that the gain of the plant correlates with the distance z_{rad}. In a first step it is assumed that z_{rad} is constant. During operation the controller should be automatically adapted to the distance so the restriction z_{rad} = const. is dropped. This adaptation to the distance is known as gain scheduling.

The controller has to fulfill several requirements for the use in laser tracker systems. First, the offset of the beam should be smaller then a quarter of the beam diameter to guarantee the interferometer function. Second, a high velocity of the reflector is necessary to allow rapid movements of the object. The third requirement is the robustness against vibrations without any disturbance of the measurement accuracy. Of course, a large measurement volume is desirable, too.

To achieve stationary accuracy the controller should possess an integrating part because the plant only consists of proportional blocks. A pure *I* controller is also possible but a proportional part enhances the performance (Merz & Jaschek 1996). A *PI* controller is well suited for plants with PT_n behavior.

A standard *PI* controller is proposed due to its simple design and to reduce the analog circuit complexity because the derivative part is missing. The transfer function is well known and given in (9).

$$H_R(s) = K_R \cdot \left(1 + \frac{1}{T_R \cdot s}\right) \qquad (9)$$

The parameter K_R describes the gain of the controller and T_R its time constant. First, these parameters are determined by the classic frequency response method as described by Föllinger (1994). The time constant T_R is set to T_x = 23.42 µs because this is the dominating time constant of the x mirror in the plant. The gain $K_{R,30°}$ is set to 0.1231 to obtain a phase margin of 30° for the gain crossover frequency. It is of interest to examine the disturbance transfer function because the set point ($w(t)$ = 0) is constant. $H_z(s)$ is calculated in (10) and is derived from the block diagram in figure 4.

$$H_z(s) = \frac{2}{1 + H_S(s) \cdot H_R(s) \cdot H_D(s)} \qquad (10)$$

To estimate the performance of the classic feedback controller the response to a ramp in $z_{lat,i}$ and the magnification factor is simulated for the disturbance transfer function in (10).

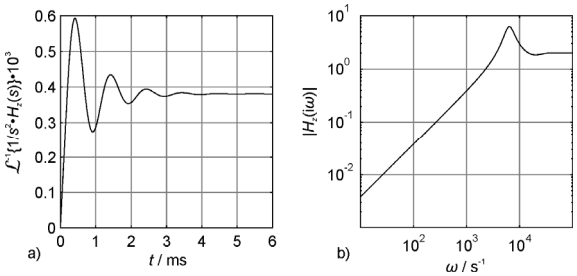

Figure 9: Simulation of the ramp response a) and the frequency response b) of the disturbance transfer function with a classic *PI* controller.

A ramp is chosen because it is the strongest requirement concerning the reflector movement. A

step is not applicable because in reality the position of the retroreflector cannot rapidly change.

Figure 9a) shows the response on a ramp in $z_{lat}(t)$ at the output y_x of the system. The maximal value of the overshoot at the output y_x is $0.60 \cdot 10^{-3}$ m until a constant contouring error of $0.38 \cdot 10^{-3}$ m is reached. Figure 9b) shows the frequency response. Low frequencies are damped due to the integrating part. But there is a magnification factor of 6.3 at a frequency of 1 kHz.

The maximal value is reached at the overshoot, but the contouring error is much lower. Therefore, the maximum of the ramp response has to be minimized so that the overshoot is reduced at the cost of the contouring error. The aim is the adaptation of the overshoot to the contouring error. For $\omega \rightarrow \infty$, $|H_z(i\omega)|$ converges to 2, so an arbitrary factor of 4 is proposed for all frequencies to guarantee robustness against vibrations. To identify the optimal controller parameters K_R and T_R were varied in a range of $K_R = 0.1 \cdot K_{R,30°} \ldots 10 \cdot K_{R,30°}$ and $T_R = 0.1 \cdot T_x \ldots 10 \cdot T_x$. The raster was $\Delta K_R = 0.05 \cdot K_{R,30°}$ and $\Delta T_R = 0.05 \cdot T_x$. Figure 10 shows the ramp response and frequency response for the optimized parameters $K_{R,opt} = 0.542$ and $T_{R,opt} = 135$ µs. The maximal value of the response is about $0.51 \cdot 10^{-3}$ m with a very low overshoot and the magnification factor does not exceed 4. So, the quality of control is much better in comparison with the classic approach.

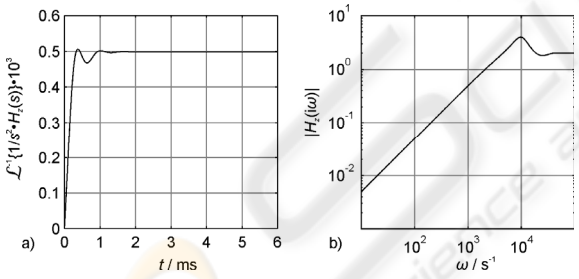

Figure 10: Simulation of the ramp response a) and the frequency response b) of the disturbance transfer function with optimal controller parameters in regard to contouring error and magnification factor.

It was assumed that the total gain is focused in the parameter K_R. This is not the case in a real system. The real total gain is a product of the controller gain, the mirror gain, the light path and the sensitivity of the quadrant diode. It can be written as

$$K_{R,opt} = K_R \cdot K_x \cdot 4 \cdot z_{rad} \cdot K_D \tag{11}$$

$$\Leftrightarrow K_R = \frac{K_{R,opt}}{K_x \cdot 4 \cdot z_{rad} \cdot K_D} \tag{12}$$

To adapt the controller gain, the parameters K_R and K_D have to be updated during operation (gain scheduling). The parameter K_D is obtained by measuring the voltage V_{Sum} of the quadrant diode. The parameter z_{rad} has to be estimated.

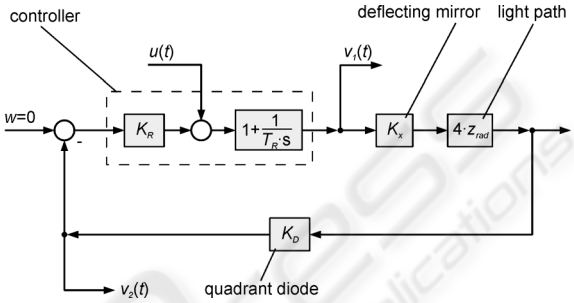

Figure 11: Control loop with introduced signal $u(t)$ to estimate z_{rad}. The signals $v_1(t)$ and $v_2(t)$ can be measured and depend on z_{rad}.

To estimate z_{rad} a known signal $u(t)$ is introduced into the control loop (figure 11). Only the spectral components are considered which are below the cut-off frequency of the diode. So, it is possible to simplify the transfer functions and consider only their proportional parts. But the time response of the controller cannot be neglected because there is a strong dependency on low frequencies introduced by the integrating part. The multiplication with z_{rad} is modeled as proportional part because z_{rad} changes slowly in comparison to the system dynamic.

The signals $v_1(t)$ and $v_2(t)$ depend on the distance z_{rad}. The transfer functions can be calculated with (13).

$$H_i(s) = \frac{\mathcal{L}\{v_i(t)\}}{\mathcal{L}\{u(t)\}}, \; i = 1,2 \tag{13}$$

It can be shown that there is a higher sensitivity of $|H_1(i\omega_0)|$ to a change in z_{rad} if signal $v_1(t)$ is measured. With (13) and figure 11 the transfer function $H_1(s)$ is calculated in (14).

$$H_1(s) = \frac{1 + \frac{1}{T_R \cdot s}}{1 + \left(1 + \frac{1}{T_R \cdot s}\right) \cdot K_R \cdot K_D \cdot 4 \cdot z_{rad} \cdot K_x} \tag{14}$$

The signal $v_1(t)$ is a superposition of the movement of the reflector and the introduced signal $u(t)$. A si-

nusoidal signal with a frequency ω_0 is proposed. So, a subsequent band-pass filter with the center frequency ω_0 suppresses the disturbance signal introduced by the reflector. To estimate the distance z_{rad} the amplitude of $u(t)$ is compared with the amplitude $v_1(t)$ and so $|H_1(i\omega)|$ is calculated. With the experimentally obtained relationship for K_D in (15), z_{rad} is calculated in (16). The proportional value m has a value of 45.13 $V^{-1}m^{-1}$.

$$K_D = \frac{m \cdot V_{Sum}}{4 \cdot K_x} \tag{15}$$

$$z_{rad} = \left(\sqrt{A^2(1-(A^2-2)T_R^2\omega_0^2 + T_R^4\omega_0^4)} - A^2T_R^2\omega_0^2\right)/\left(A^2K_R m V_{Sum}(1+T_R^2\omega_0^2)\right) \tag{16}$$

with $A = |H_1(i\omega_0)|$.

To obtain an appropriate value for the amplitude of the signal $u(t)$ the beam deviation $y_x(t)$ from the center of the quadrant diode is analyzed. The deviation should be smaller than a quarter of the beam diameter to guarantee the interferometer function. During distance estimation the deviation $y_x(t)$ is a superposition of the lateral movement of the reflector $z_{lat,x}(t)$ and the introduced signal $u(t)$. Therefore, the amplitude of the signal $u(t)$ is chosen to be only 10% of the maximal deflection so that the maximal velocity v_{lat} is not reduced. With the transfer function $H_2(s)$ and a maximal amplitude $y_{x,max}$ of $y_x(t)$ the amplitude u_0 is calculated in (17).

$$u_0 = y_{x,\max} \cdot \frac{K_D}{|H_2(i\omega_0)|} \tag{17}$$

Because z_{rad} is located in the denominator of (17) its increase leads to a decreasing amplitude u_0. According to the described limit of 10%, $y_{x,max}$ is set to *R/20* with *R* being the radius of the beam.

5 PRACTICAL CONSIDERATIONS

The feedback controller is implemented in an analog design. To generate the signal $u(t)$, to measure the signal $v_1(t)$ and to adapt the gain of the controller, a microcontroller is used. The microcontroller is an ATmega128 and is programmed in C. The variable gain control is realized by digital potentiometers that are set by the microcontroller. Figure 12 shows the used circuit for one axis. The digital potentiometer R_2 offers 127 linearly arranged steps. The resistance can be adjusted between 1 kΩ and 50 kΩ.

The analog *PI* controller is built with standard components without complex serial or parallel circuits resulting in a time constant of T_R = 132 µs and a adjustable gain between $K_R = 6.00 \cdot 10^{-3} \ldots 300 \cdot 10^{-3}$. The parameter T_R remains constant even if the potentiometers change their value. Because of the discrete potentiometer positions there is an error between the optimal controller gain and the achieved controller gain. There are only integer positions n_{int} available. To obtain an optimal value for K_R the theoretical real number n_{real} for the potentiometer position is calculated. Afterwards, n_{real} is rounded down and up and the lower and the upper controller gains K_l and K_u are calculated. The controller gain with the minimal error in regard to the optimal value is chosen.

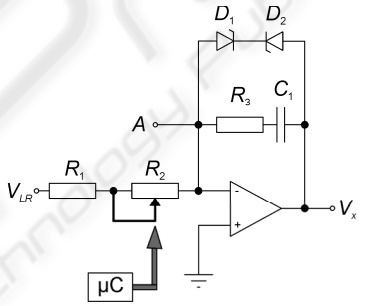

Figure 12: Microcontroller controlling a digital potentiometer and analog *PI* controller exemplarily shown for the x-axis.

After power up sequence and beam loss during operation, the laser beam searches the reflector in a defined area. This is done by deflecting the mirrors of the actuator without opening the feedback loop. The influence of the analog part is reduced and only the digital part controls the mirror deflection.

Figure 13 shows the operation principle. The digital potentiometer is set to its maximal value. So, the influence of the sensor signal to the input of the *PI* controller is weak. This is comparable to an opening of the feedback loop and the signal can be cross talked easily.

The microcontroller introduces a signal at the input of the *PI* controller. At the same time the reduced sensor signal of the diode acts as a disturbance variable. The output of the controller is digitalized and is compared to the set up variable w_α. The microcontroller multiplies the gain K_μ with the deviation *e*. So, the plant with integrating behavior is controlled via a *P* controller which is a good combi-

nation (Merz & Jaschek 1996). The DA conversion at the output of the microcontroller is done via a pulse width modulation (PWM) with a frequency of 14.4 kHz and a low-pass filter with a cut-off frequency of 300 Hz (smoothing function).

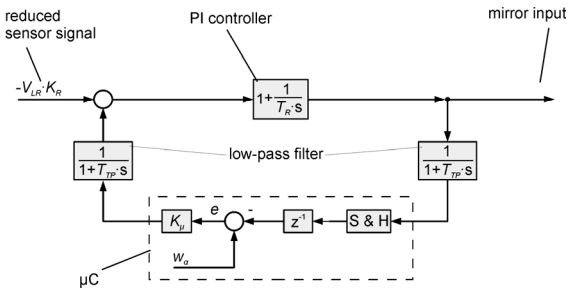

Figure 13: Operation principle for deflecting the mirrors in a defined way.

The output of the controller is digitized by the integrated AD converter of the microcontroller. To reduce alias effects a low-pass filter with a cut-off frequency of 300 Hz is used, too.

K_μ represents the total gain of the control loop and is set to $K_\mu = 41$. This is a tenth of the value of the stability limit. So, the safety margin is high enough to avoid instability.

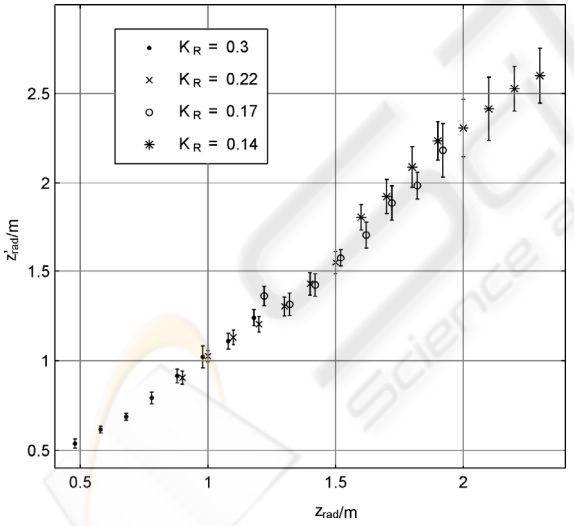

Figure 14: Estimated z'_{rad} as a function of the real z_{rad}. Each point is averaged 20 times with its two-time standard deviation. To increase readability the measurements for $K_R = 0.3$ show a horizontal offset of -0.02 m and for $K_R = 0.17$ an offset of +0.02 m.

To estimate the distance z_{rad} between the system and the retroreflector a signal is introduced in the x-axis (figure 11). To reduce the computing and programming complexity a square wave with a frequency of 200 Hz instead of a sinusoidal signal is used. An analog band pass filter with the same frequency is used for signal pre-processing. Only the basic frequency is considered in the signal analysis. Because the movement of the retroreflector has only few spectral components in the pass-band the gain can be increased without leaving the input range of the AD converter. So, a small value of u_0 is sufficient to detect the amplitude of $v_1(t)$ with a DTFT.

Figure 14 shows the distance estimation for different gains of the controller. To reduce the time effort only distances between 0.5 m and 2.3 m are measured. The estimated value shows a good accordance to the real values. The variance increases with the distance because of the reduced sensitivity of the measured voltage to the distance.

Further experiments have shown that the retroreflector can be moved with a maximal velocity of $v_{max} = 2.5$ m/s at unlimited acceleration and a beam offset of a quarter of the beam diameter. Distances between 0.5 m and 7.8 m (length of laboratory) were tested without tracking problems.

6 CONCLUSIONS

An analog *PI* controller with additional features was presented for the use in laser tracker systems. It is fast to detect a rapid beam movement and shows good control accuracy. Functions as gain scheduling and distance estimation are integrated in this hybrid design consisting of a digital and analog part.

REFERENCES

Föllinger, O., 1994. *Regelungstechnik.* 8th ed. Heidelberg: Hüthig GmbH.

Merz, L. & Jaschek, H., 1996. *Grundkurs der Regelungstechnik.* 13th ed. München/Wien: R. Oldenburg Verlag.

Riemensperger, M. & Gottwald, R., 1990. Kern Smart 310 – Leica's Approach to High Precision 3D Coordinate Determination, In: *F. Löffler*, *2nd International Workshop on Accelerator Alignment*. Hamburg, Germany, 10-12 September 1990. pp. 183-200.

Schwarze, G., 1962. Bestimmung der regelungstechnischen Kennwerte von P-Gliedern aus der Übertragungsfunktion ohne Wendetangentenkonstruktion, *Messen, Steuern, Regeln,* 5, pp. 447-449.